

Laser effect in the optical luminescence of oxides containing Cr

¹Iveta Malíčková, ¹Jana Fridrichová, ^{1,2}Peter Bačík, ³Stanislava Milovská, ⁴Radek Škoda, ⁵Ludmila Illášová, ⁵Ján Štubňa

¹Department of Mineralogy and Petrology, Faculty of Natural Sciences, Comenius University in Bratislava, Ilkovičova 6, SK-842 15 Bratislava, Slovakia; malickova3@uniba.sk

²Earth Science Institute of the Slovak Academy of Science, Dúbravská cesta 9, SK-840 05 Bratislava, Slovakia

³Earth Science Institute of the Slovak Academy of Science, Ďumbierska 1, SK-974 01 Banská Bystrica, Slovakia

⁴Department of Geological Sciences, Masaryk University, Kotlářská 2, CZ-611 37 Brno, Czech Republic

⁵Gemological Institute, Faculty of Natural Sciences, Constantine the Philosopher University in Nitra, Nábřežie mládeže 91, SK-949 74 Nitra, Slovakia

AGEOS

Abstract: Laser has dual role in mineralogy; minerals are used as a source of laser radiation and laser is employed in mineral analytical study. Therefore, we used spectroscopic methods to study Cr-bearing minerals, which are potential laser sources. Chemical composition was determined by XRF analysis, and shows that ruby is enriched in Fe, Ti and Cr, alexandrite contains Ti, Cr, Fe, Mg, Ca, and Si, spinel has increased Si, Cr, V, Fe, and Ca, and uvarovite contains Ti, V, Fe, and Mn along with major Cr. The luminescence spectra of ruby samples measured by Raman spectrometer have two very narrow and intense bands between 690 and 698 nm. Alexandrite has a broad luminescence band in the 640 – 780 nm region and has two intense bands at 680 and 710 nm. The spinel luminescence bands occur in the region ranged from 673 to 725 nm, are broader than in ruby, but still intensive. Uvarovite has a broad band in the region between 655 and 950 nm. Strong luminescence emission in ruby at about 695 nm and in alexandrite between 640 and 780 nm can be attributed to the laser effect – spontaneous emission due to the energy transition from metastable E to basic A₂ state. This is also manifested in the optical spectra; there is an intensive transmission in the spectral region, where the luminescence laser effect occurred.

Key words: corundum, ruby, laser-effect, Raman spectroscopy, luminescence

1. INTRODUCTION

Light Amplification by Stimulated Emission of Radiation (LASER) is a radiation source of coherent electromagnetic energy with the high intensity of radiation. Robert von Lieben and Lee de Forest constructed a vacuum amplifier tube in 1905–1906. The tube could amplify electromagnetic waves in a wide range of wavelengths. They also created an oscillator which could generate such waves. Until 1950, heat sources were mostly used to generate electromagnetic waves in the optical frequency band. Generation of coherent optical waves (Fig. 1C) was possible only by laser (Siflvast, 2014).

The first amplifier based on discrete energy levels (quantum amplifier) was MASER (Microwave Amplification by Stimulated Emission of Radiation) invented by Gordon, Townes and Zeiger in 1954 (Bertolotti, 2015). In 1958, Schawlow and Townes proposed to extend the MASER principle to an optical mode. Enhancement should take place from stimulated emission between individual energy levels, which must be inverse. Amplifiers

and oscillators are based on the stimulated emission principle, called LASER (Schawlow & Townes, 1958; Svelto, 2010). The first functional laser was built in 1960 by Teodor Mainman. It was a ruby laser with a 694.3 nm wavelength (Mainman, 1960). Compared to present lasers, it was simple and imperfect because it used only three energy levels of the ruby crystal and therefore could only work in a pulse mode. N. G. Basov, A. M. Prochorov and Ch. H. Townes eliminated this problem by using multiple energy levels (Svelto, 2010).

Lasers are widely used in various fields of science, technology, medicine, art, cultural heritage, cosmology, spectroscopy and atomic physics. Optical methods and techniques use lasers as light sources for various cultural heritage diagnostics (e.g., holographic interferometry, Raman spectroscopy, 3D laser scanning) (Ristic et al., 2010).

In this study, we would like to emphasize dual role of laser in mineralogy. As the first laser, the ruby crystal was used and this effect was later discovered and utilized in more minerals. The second role is in the use of laser for spectroscopic investigation

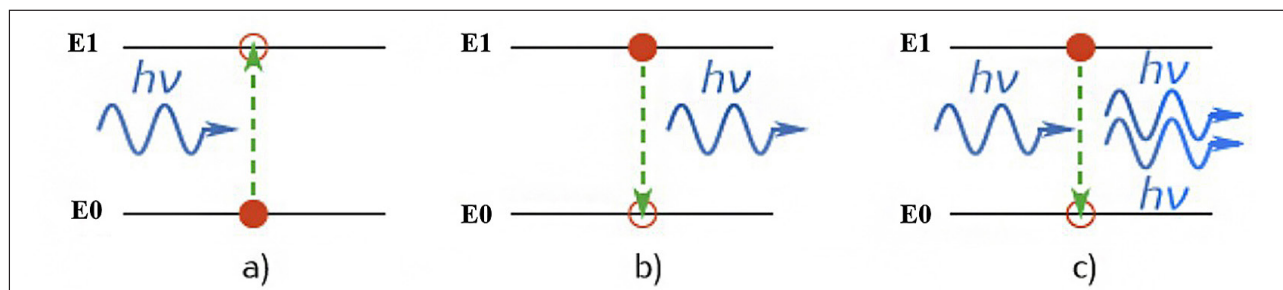


Fig. 1. Interaction scheme (a) absorption (b) spontaneous emission (c) stimulated emission (Svelto, 2010, modified).

of minerals, where the laser is employed to determine mineral characteristics. Therefore, we studied Cr-bearing minerals which are potential laser sources with spectroscopic methods. We studied ruby and alexandrite as known laser sources but we included other Cr-rich minerals as spinel and uvarovite which could also produce coherent light waves but are not usually widely used.

2. LASER PRINCIPLE

The laser is a monochromatic coherent light source that is created by placing a light amplifier in an optical resonator tuned to the appropriate wavelength (Mainman, 1960). This is the phenomenon of the photon interaction with the atom or molecule. We distinguish the three basic types of interactions – absorption, spontaneous and stimulated emission (Fig. 1) (Svelto, 2010).

When considering the two energy levels, E_0 and E_1 , where E_0 is a ground level (quantum state of minimal energy), then $E_0 < E_1$. The atom with E_0 energy level tends to remain at the ground level until energy is delivered (action and reaction). The energy supply (electromagnetic wave represented by photons) is accompanied by the energy state change. If the photons energy is equal to the difference $E_1 - E_0$, the atom absorbs this energy and changes to E_1 , thus the radiation is absorbed. Since $E_0 < E_1$, the atom tends to pass to a more energy efficient level – E_0 . The transition to the ground level causes energy reduction $E_1 - E_0$, if the energy is emitted as electromagnetic radiation, it is spontaneous emission, which is expressed by the equation $h\nu = E_1 - E_0$ (h is Planck constant, ν is the frequency of released radiation). If the atom occurs on E_1 and the electromagnetic wave with frequency ν (frequency of spontaneously emitted radiation) is impacted at the same time, then the incident wave forces the atom to pass into E_0 . The transition is accompanied by the radiation emission with $h\nu$ energy. Waves (both incident and emitted) have the same direction and are in phase which results in an amplification of the original radiation – stimulated emission. In order to have a continuous stimulated emission, there must be an excess of inverse particles (population inversion – there

is a thermodynamic equilibrium violation when higher energy states have more photons than the ground level, otherwise they are absorbed) at higher energy levels compared to lower ones. Otherwise, the lower levels particles would absorb released energy (Svelto, 2010).

In the case of the 3-level system (Fig. 2A), E_0 is the ground state and E_2 is the excited state. With a sufficient energy supply in the form of electromagnetic radiation, electrons reach E_2 , and subsequently descend to E_1 level without emission (inverse population can occur). The individual transitions between the energy levels are variously fast, there is a very fast transition between E_2 and E_1 (resulting in free states on E_2) but the transitions are very slow between E_1 and E_0 because E_1 must be metastable to reach an increased population (Penzkofer, 1988).

In the 4-level system (Fig. 2B) there is an inverse population between two excited states, E_2 and E_1 . Energy supply to the electrons will cause their transition to E_3 . Internal conversion causes a rapid decline to a metastable level E_2 where electrons accumulate. The stimulated electron emission is formed between E_2 and E_1 levels. Subsequently, rapid electron decomposition occurs between E_1 and E_0 (Penzkofer, 1988).

The laser system consists of a pumping device, an optical resonator, a lasing medium (Fig. 3). The medium can be ruby, Nd: YAG (Y-Al garnet), Ti-sapphire, HeNe, CO_2 , organic dyes (Rhodanin) (Tab. 1). The pumping system (the excitation system) supplies the necessary energy to the lasing medium, there is a particle excess at the higher energy levels. It provides the inverse population necessary for stimulated emission. The optical resonator consists of two parallel mirrors; one is partially reflective, used to achieve a higher number of inverse populations. The pumping system supplies energy to the medium. Radiation leaves the medium and reflects from the mirror back causing further stimulated emission. This process is repeated until the laser radiation has the required intensity, and after reaching the maximum intensity, the beam leaves resonator through the partially reflective mirror (Black & Jobling, 2014).

3. MATERIALS AND METHODS

We studied five natural samples from the following localities (abbreviations are shown in the brackets): ruby (corundum) from Madagascar (RMA-1), ruby (corundum) from Mozambique – Montepuez (RMO-1), alexandrite (chrysoberyl) from Tanzania – Lake Manyara (ALM-1), spinel from Myanmar – Mogok (SPM-1), uvarovite (garnet) from Russia – Sarany, Ural (UVU-1). All samples were crystal fragments of various shapes and sizes and several of them had gemmological quality (Fig. 4).

Raman spectroscopy was performed by LabRAM-HR Evolution (Horiba Jobin-Yvon) spectrometer system with a Peltier cooled CCD detector and Olympus BX-41 microscope (Masaryk University, Department of Geological Sciences). Raman spectra were excited by 473 nm frequency-doubled diode laser and a 520.6 cm^{-1} silicon wafer enabled spectral calibration. Spectra ranged from 100 to $10\,000 \text{ cm}^{-1}$ with acquisition time of 10 s per frame and 2 accumulations.

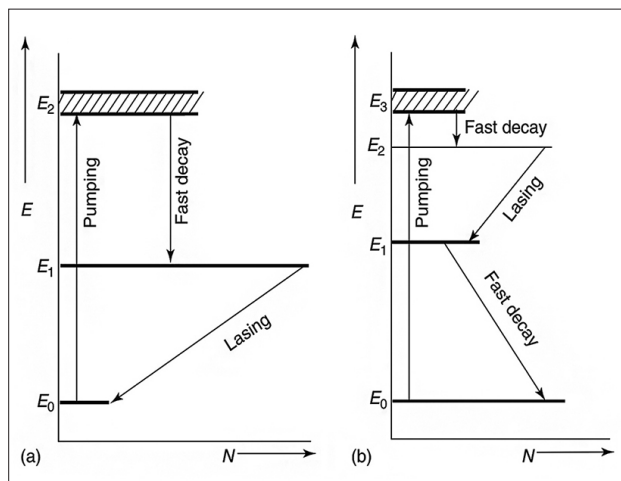


Fig. 2. Three level system (a) and four level system (b) (Singh et al., 2012).

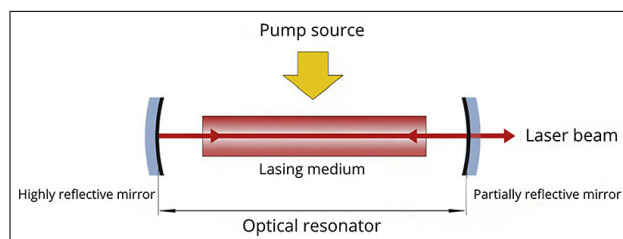


Fig. 3. Basic components of laser (Black & Jobling, 2014, modified).

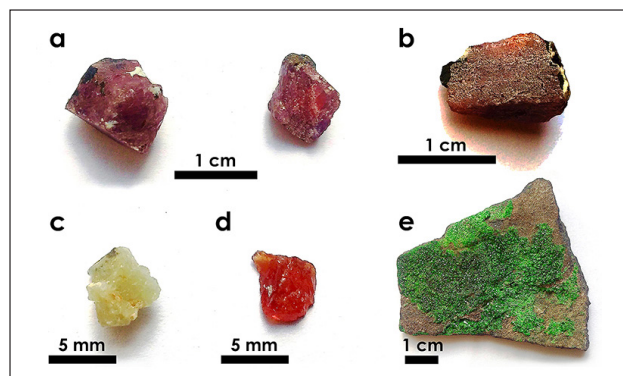


Fig. 4. Photographs of samples: ruby (a – RMA-1, b – RMO-1), alexandrite (c), spinel (d) and uvarovite (e).

Optical absorption spectra of samples in the region (400–750 nm) were measured with the GL Gem SpectrometerTM at room temperature in the Gemological Institute of Constantine the Philosopher University, Nitra.

Both Raman and UV/Vis/NIR spectra were processed in Seasolve PeakFit 4.1.12 software. Raman and absorption bands were fitted by Lorentz function with automatic background correction and Savitzky-Golay smoothing.

Chemical composition (Tab. 1) was determined by micro X-ray fluorescence spectroscopy (micro-XRF) using an

instrument M4 TORNADO, Bruker (Earth Science Institute of the Slovak Academy of Science, Banská Bystrica). Incident X-ray beam (Rh anode) was focused by polycapillary optics to 25 micron spot, interaction depth was ca. 10–1000 μm , excitation current 600 μA at 50 kV. Analyses were acquired at 20 mbar vacuum. A silicon drift detector (SDD) collecting the fluorescence signal has an active area 30 mm^2 and spectral resolution 145 e. Measuring time of point analyses was 70 s, live time 60 s, energy range of 0.25–20 keV. Element concentrations were computed by fundamental parameters method.

4. RESULTS

The samples were identified by Raman spectroscopy and compared to the RRUFF database (Fig. 5).

Results obtained from XRF analysis (Tab. 2) were not converted to crystal-chemical formula, but were reported in wt. %

Tab. 2. Results of X-ray fluorescence analysis of the studied samples.

	RMA-1 (wt. %)	RMO-1 (wt. %)	ALM-1 (wt. %)	SPM-1 (wt. %)	UVU-1 (wt. %)
SiO ₂	7.25	10.42	0.14	0.79	20.14
TiO ₂	0.03	0.03	0.81	0.07	0.84
Al ₂ O ₃	88.56	85.77	90.28	68.36	4.47
Cr ₂ O ₃	0.18	0.80	0.72	3.96	23.09
V ₂ O ₃	0.01	0.00	0.00	0.63	0.11
FeO	1.38	1.40	2.63	0.15	0.59
MnO	0.01	0.00	0.00	0.02	0.10
MgO	0.02	0.06	0.31	24.23	0.00
CoO	0.01	0.01	0.02	0.00	0.01
NiO	0.00	0.00	0.04	0.01	0.01
SrO	0.01	0.02	0.02	0.02	0.02
CaO	0.70	0.27	0.71	0.50	44.88

Tab. 1. Basic classifications of lasers (Singh et al., 2012).

Depending on the nature of the active media		
Gas	atomic laser	He-Ne, He-Cd, Cu, I
	ion laser	Ar, Kr
	molecular laser	CO ₂ , N ₂ , H ₂
	excimer laser	XeBr, KrO, ArO
Solid state	Nd: YAG, Nd: sklo, Er:YAG, Yb: YAG, Ti sapphire, ruby	
Semiconductor	GaAs, GaN, PbSnSe, InAsSb	
Dye/Liquid laser	Organic dyes: rhodanin, styryl, LDS, coumarin, rhodamine, stilbene	
Depending on the wavelenght		
Infrared (780 nm – 1 mm)		
UV/Vis (360–780 nm)		
Ultraviolet (10–360 nm)		
Depending on the mode of work		
Continuous wave	stable beam generation	
Single pulsed	normal mode	
Q-Switched	high energy pulses	

because the measured data did not have sufficient precision to calculate the stoichiometric formula. The most abundant element in the ruby samples (RMA-1, RMO-1) is Al; ruby is also enriched in Fe, Ti, and Cr. Chromium substitutes for aluminium and causes red colour. Other elements such as Si are probably bound in the form of microscopic impurities. In alexandrite sample (ALM-1) the Al is the most represented (Be is not analysed), Ti, Cr, Fe, Mg, Ca, and Si occur in a smaller amount. The highest Al and Mg content were measured in spinel (SPM-1), corresponding to the mineral formula, Si, Cr, V, Fe, and Ca amount is increased. It indicates Cr-enriched spinel. In uvarovite sample (UVU-1), the most abundant octahedral cation is Cr; Ti, V, Fe, and Mn occur in increased amounts. Chromium is directly based in the structural formula of uvarovite and therefore, the Cr content in uvarovite is the highest from all the samples where Cr occurs as a substituent.

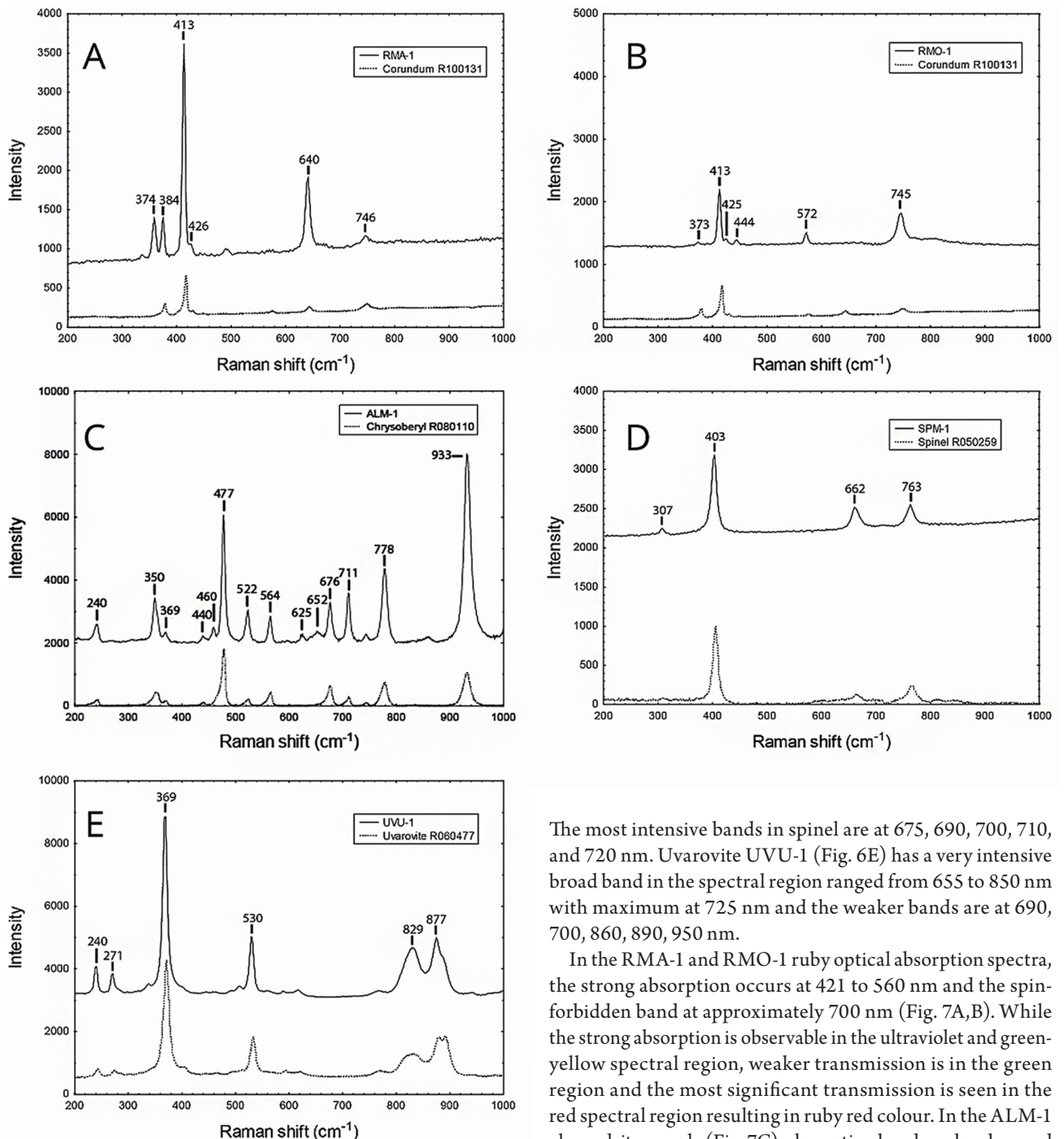
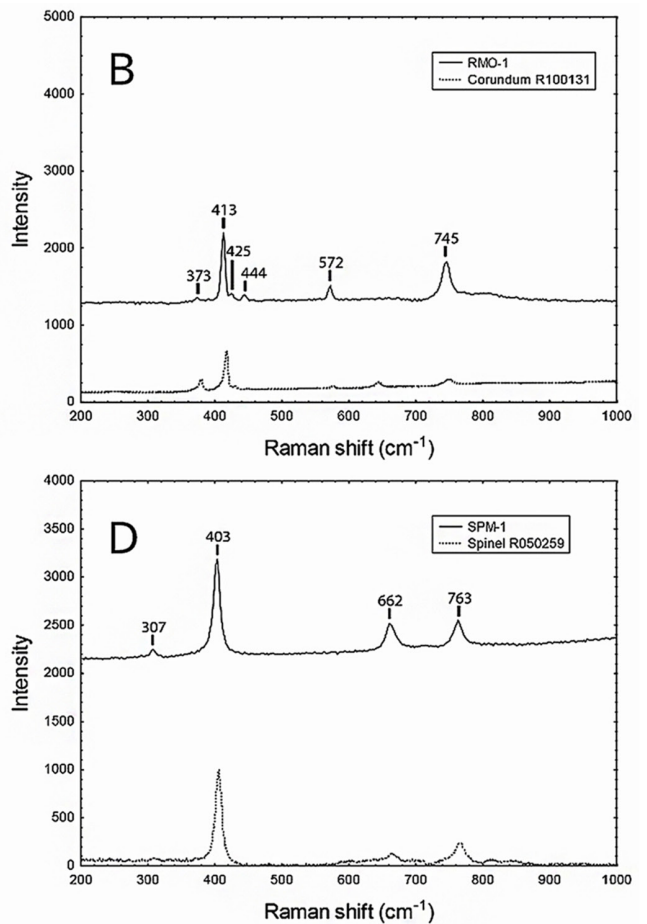


Fig. 5. Raman spectra of ruby (A, B), alexandrite (C), spinel (D) and uvarovite (E), compared to the RRUFF database.

The luminescence spectrum of ruby RMA-1 (Fig. 6A) has very narrow and intense bands, in RMA-1 sample the most intensive split band is in the 690 and 698 nm regions. The RMO-1 sample (Fig. 6B) has the most significant band in the region ranged from 693 to 697 nm. Alexandrite ALM-1 (Fig. 6C) has a broad luminescence band in the 640–780 nm region and has two intense bands at 680 and 710 nm. The spinel SPM-1 luminescence bands (Fig. 6D) occur in the region ranged from 673 to 725 nm, are broader than in ruby, but still intensive.



The most intensive bands in spinel are at 675, 690, 700, 710, and 720 nm. Uvarovite UVU-1 (Fig. 6E) has a very intensive broad band in the spectral region ranged from 655 to 850 nm with maximum at 725 nm and the weaker bands are at 690, 700, 860, 890, 950 nm.

In the RMA-1 and RMO-1 ruby optical absorption spectra, the strong absorption occurs at 421 to 560 nm and the spin-forbidden band at approximately 700 nm (Fig. 7A,B). While the strong absorption is observable in the ultraviolet and green-yellow spectral region, weaker transmission is in the green region and the most significant transmission is seen in the red spectral region resulting in ruby red colour. In the ALM-1 alexandrite sample (Fig. 7C), absorption band can be observed at 440, 586, and 850 nm. Significant absorption is in ultraviolet, yellow and near infrared spectral region. Transmission occurs in the green and red region. The resulting alexandrite colour is green. The SPM-1 spinel optical absorption bands (Fig. 7D) are at 454, and 551 nm. Significant absorption is observed in the ultraviolet, and yellow region, the weak transmission is seen in the green region, but the most significant transmission is in the red region. The resulting spinel colour is red. Uvarovite UVU-1 (Fig. 7E) has optical absorption bands at 463, 572, 689 nm. Significant absorption is observed in blue, yellow-green and red region. Transmission is in the green and near infrared region and the resulting colour of the uvarovite is green.

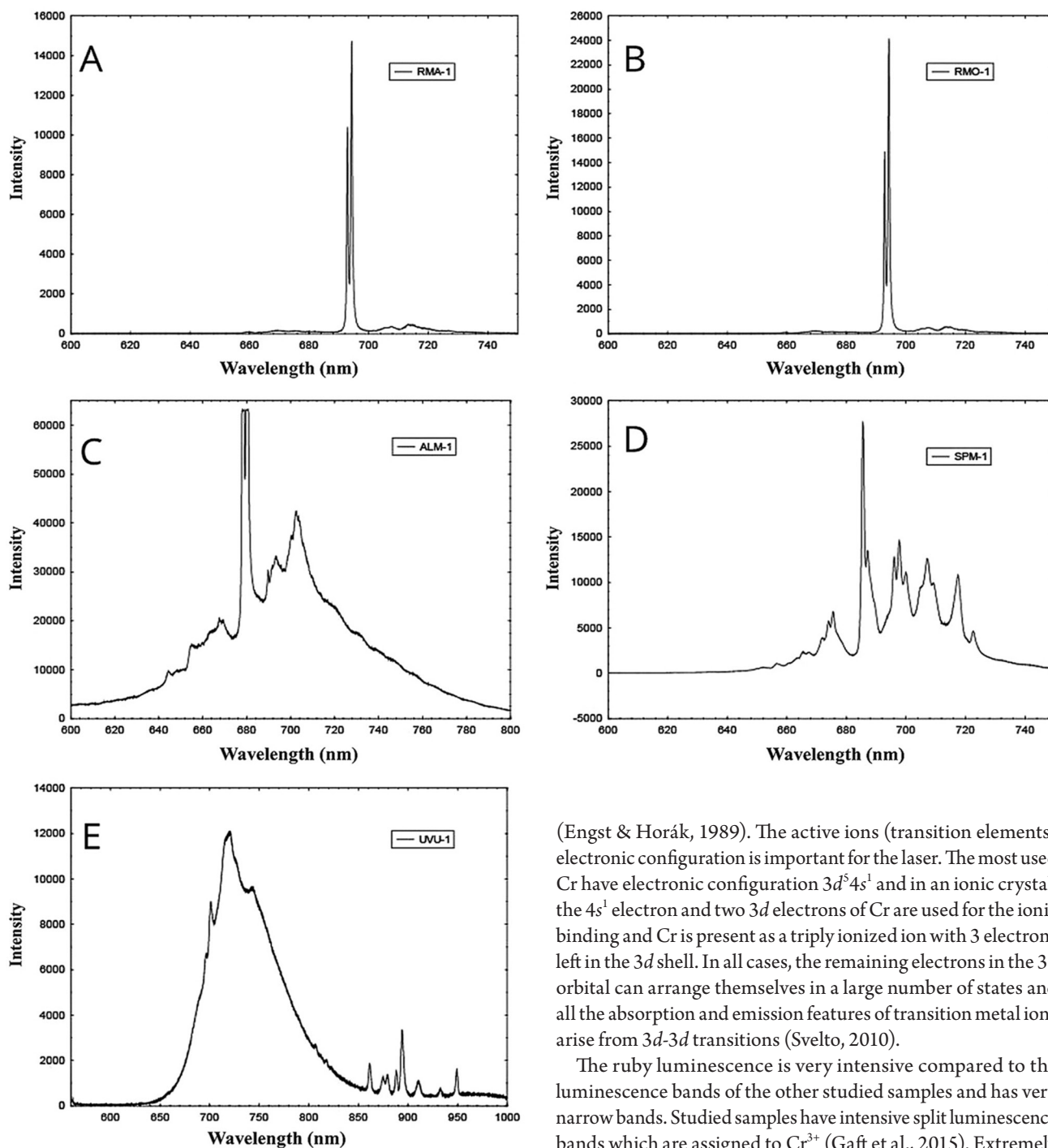


Fig. 6. Luminescence spectra of ruby (A, B), alexandrite (C), spinel (D) and uvarovite (E).

5. DISCUSSION

The laser effect can be observed in luminescence spectra, where intensive emission occurs. To reach the laser effect, the specimen needs to be doped with active ions. In the crystalline substances, the active ions are incorporated into the crystal structure and have a fixed orientation in the structural force field. For the active ion doping, mostly used are REE ions (Nd^{3+} , Sm^{2+} , Tm^{3+} , Pr^{3+} , and others), or 4A subgroup elements, mainly Cr^{3+} and U^{3+}

(Engst & Horák, 1989). The active ions (transition elements) electronic configuration is important for the laser. The most used Cr have electronic configuration $3d^5 4s^1$ and in an ionic crystal, the $4s^1$ electron and two $3d$ electrons of Cr are used for the ionic binding and Cr is present as a triply ionized ion with 3 electrons left in the $3d$ shell. In all cases, the remaining electrons in the $3d$ orbital can arrange themselves in a large number of states and all the absorption and emission features of transition metal ions arise from $3d$ - $3d$ transitions (Svelto, 2010).

The ruby luminescence is very intensive compared to the luminescence bands of the other studied samples and has very narrow bands. Studied samples have intensive split luminescence bands which are assigned to Cr^{3+} (Gaft et al., 2015). Extremely increased intensity of ruby luminescent bands is associated with a laser effect that occurs at 695 nm. The red light is radiated from the ruby when the crystal is illuminated with green, violet or ultraviolet light. The ruby laser has three energy levels that are excited, metastable and ground state level. If the system contains all three energy levels (Fig. 8), the photons are weakly vibrated at low temperature and remain at the ground state. When temperature increases, thermal vibrations of the photons occur and can excite electron to a metastable level (absorption occurs), then returns to the ground state (emission occurs) at a very slow velocity of 10^{-7} s typical for ruby. Subsequent temperature increasing leads to higher energy levels occupation, which causes the reduction at the ground state. The endless

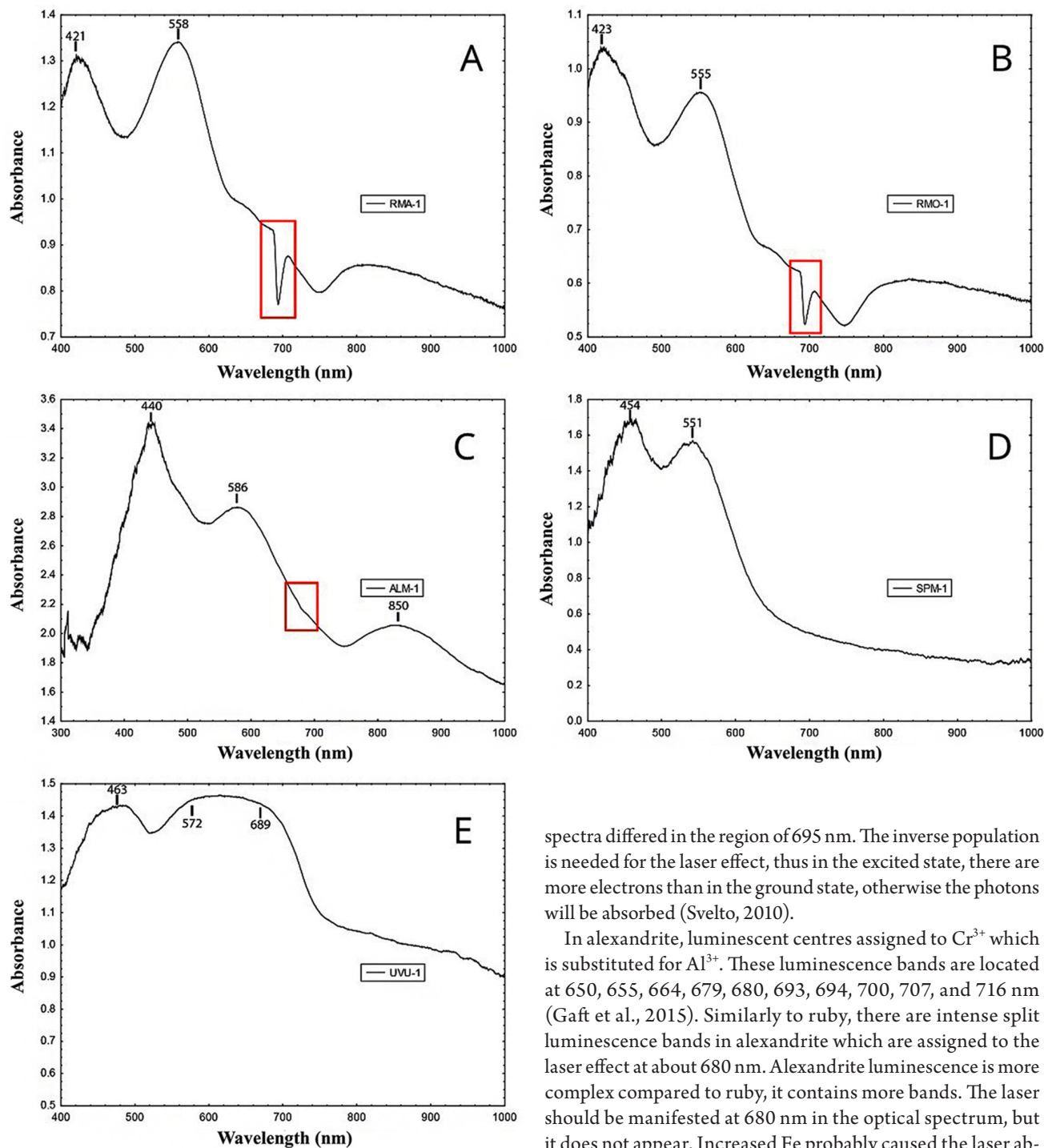


Fig. 7. Optical absorption spectra of ruby (A, B), alexandrite (C), spinel (D) and uvarovite (E).

The Cr presence in the ruby structure is the main cause of its colour (up to 4%). Trivalent chromium has two distinct absorption bands in the visible spectrum – in violet and green region, so the resulting ruby colour is red; different red shades or hues are associated with impurities such as Fe^{3+} and V^{3+} (Gaft et al., 2015). The spin-forbidden band for absorption occurs in the region at 695 nm, and is associated with the ruby laser (Rossman, 2017). We studied two different ruby samples, whose optical

spectra differed in the region of 695 nm. The inverse population is needed for the laser effect, thus in the excited state, there are more electrons than in the ground state, otherwise the photons will be absorbed (Svelto, 2010).

In alexandrite, luminescent centres assigned to Cr^{3+} which is substituted for Al^{3+} . These luminescence bands are located at 650, 655, 664, 679, 680, 693, 694, 700, 707, and 716 nm (Gaft et al., 2015). Similarly to ruby, there are intense split luminescence bands in alexandrite which are assigned to the laser effect at about 680 nm. Alexandrite luminescence is more complex compared to ruby, it contains more bands. The laser should be manifested at 680 nm in the optical spectrum, but it does not appear. Increased Fe probably caused the laser absence (Pugh-Thomas et al., 2010) and also a slight decrease in spectrum intensity at 680 nm in alexandrite. Overall, we can conclude that Fe presence in alexandrite can cause distortion of optical spectrum compared to published data (Rossman, 2017; Trindade et al., 2010). The active ions (Cr^{3+}) in alexandrite are obtained in the excited state. Consequently, the ions lose their energy and pass to a lower energy metastable level. The stimulated emission of electrons appears between 2 and 1 level (Fig. 9) (Gusch & Jones, 1982).

For the comparison, the ruby has three energy levels and alexandrite has four energy levels; therefore its laser is more efficient than in ruby. Obtaining an inverse population in ruby is

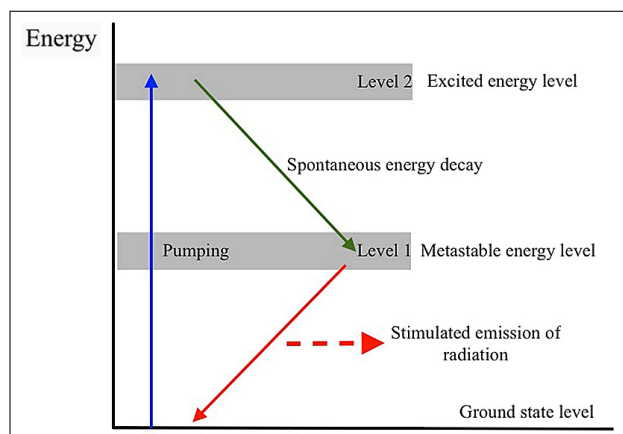


Fig. 8. Energy levels in ruby laser (Khanin, 1995, modified).

comparatively more difficult than in alexandrite. In the ruby, laser photons are released between E1 and E0. At the four-level system of alexandrite, the inverse population is easily reached between E2 and E1, since E1 depopulates the electrons, and laser photons release occurs between E2 and E1 (Fig. 10). The advantage of the alexandrite laser is a continuous vibration E1 level band covering a wide energy area (allowing laser tuning to a wide range of wavelengths) (Hollas, 2004). Photons have a short lifetime at higher energy levels and a rapid transition to lower energy states causes inverse population. This difference causes stimulated emission between E2 and E1 levels and the subsequent photons decrease to the ground energy state (Yorulmaz et al., 2014).

When comparing the optical and luminescence spectra, there is a similar laser effect, the difference is only in the band orientation. There is a strong absorption of radiation between the transitions. Conversely, some transitions between energy levels are spectroscopically undetectable, they are forbidden. In the case of forbidden transitions in ruby, there is no photon absorption or emission at 700 nm. However, there can still be the energy transition and atom can release energy in the form other than the emission, such as atom vibrations. Other transitions involving absorption and emission are called allowed transitions (Engst & Horák, 1989).

If luminescence is present, emission occurs in ruby at about 695 nm, and in alexandrite between 640 and 780 nm. This is also manifested in the optical spectra; there is an intensive transmission in the spectral region, where the luminescence laser effect occurred. Intensive luminescence bands in ruby and alexandrite are attributed to spontaneous emission due to the energy transition from metastable E to ground A₂ state (Figs. 8, 9) (Yorulmaz et al., 2014).

We used spinel and uvarovite as comparative samples. In our study, we have a red-coloured spinel which colour is caused by Cr³⁺ at an octahedral site (Fritsch & Rossman, 1988). Spinel has a more complex structure than ruby and alexandrite, with two cation sites. Its complexity is also visible in the luminescence spectrum, which contains several bands. Luminescent bands were assigned to Cr³⁺ at 676, 686, 698, 708, and 718 nm and are consistent with published data (Gaft et al., 2015). The partial stimulated emission showed at 698 nm. Spinel colour is caused by Cr³⁺, Fe²⁺, Fe³⁺, and Co²⁺.

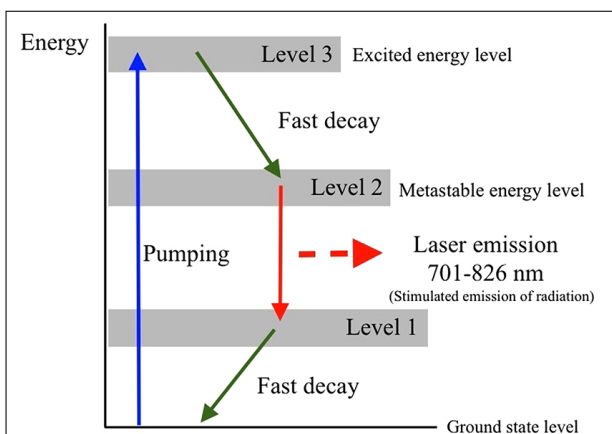


Fig. 9. Energy levels in alexandrite (Khanin, 1995, modified).

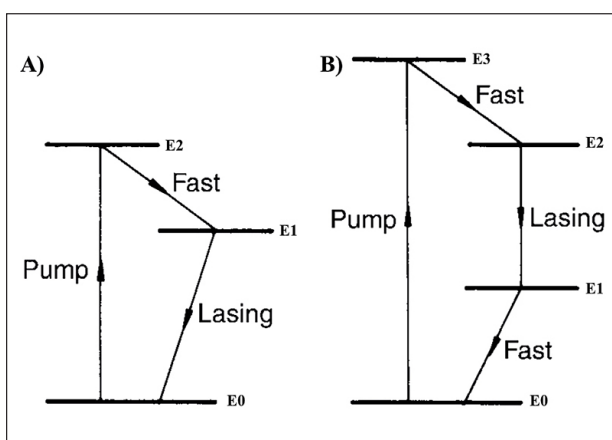


Fig. 10. Simplified model of energy levels A) ruby a B) alexandrite (Hollas, 2004).

There is no observable laser effect in spinel optical spectra, although spinel can be used as a laser material in optical technologies. The spinel needs to be doped by active ions: Cr³⁺ for use in solid-state lasers, and Fe³⁺, Mn²⁺ for fiber-optic thermometers (replacing ruby crystal), which was studied for their potential use in short wavelength solid lasers (Jouini, 2007).

Uvarovite has a green colour caused by the Cr³⁺ confirmed by chemical analysis. Our analysis is well consistent with published data (Fritsch & Rossman, 1988). The garnet colour is caused by the Cr³⁺, V³⁺, Fe³⁺ presence at the octahedral sites, and the Fe²⁺ presence in polyhedral site, Fe²⁺-Ti⁴⁺ charge transfer can affect the garnet spectrum. The green colour of uvarovite is due to Cr. When comparing the luminescence spectra, the uvarovite spectrum is different; the luminescence band is wider and higher than in other studied samples. Optical spectrum of uvarovite also does not contain any indication of laser effect.

6. CONCLUSION

The laser technology makes a progress and possibilities to use are constantly being developed. Materials suitable to the laser are

various including ruby, alexandrite, spinel and even diamond. The laser effect is dependent on the chemical composition of material used for laser production. Admixtures in materials used in lasers cause spectral distortion and decrease the efficiency of the laser effect in minerals.

Ruby is the most commonly used in lasers; the laser effect occurs on a spin-forbidden band. Alexandrite is also suitable for laser but should be without impurities. Research on the spinel use in lasers is currently underway for various purposes.

In conclusion, the sample suitable for laser use must fulfil specific conditions – structural properties, chemical composition. To produce a laser effect, sample has to contain sufficient active ions or to be doped with them.

Acknowledgments: We thank R. Hanus and P. Antal for their detailed reviews which improved the quality of our work. This work was supported by the Slovak Research and Development Agency under the contracts No. APVV-15-0050 and APVV-17-0134, and the Ministry of Education of Slovak Republic grant agency under the contracts VEGA-1/0079/15 and VEGA-1/0499/16.

References

- Bertolotti M., 2015: Masers and Lasers. Second Edition: An Historical Approach. CRC Press, 502 p.
- Black S. & Jobling L., 2014: Physical principles of LASER. *Anaesthesia & Intensive Care Medicine*, 15, 11, 530–532.
- Engst P. & Horák M., 1989: Aplikace laserů [Laser application]. SNTL-Státní Nakladatelství Technické Literatury, Praha, 34, 204 p. [in Czech]
- Fritsch E. & Rossman G.R., 1988: An update on color in gems. Part 3: Colors caused by band gaps and physical phenomena. *Gems & Gemology*, 24, 2, 81–102.
- Gaft M., Reisfeld R. & Panczer G., 2015: Modern Luminescence Spectroscopy of Minerals and Materials. Springer, 606 p.
- Gusch S.Jr. & Jones C.E., 1982: Alexandrite-laser performance at high temperature. *Optics Letters*, 7, 12, 608–610.
- Hollas J.M., 2004: Modern Spectroscopy, Fourth edition. Wiley, 452 p.
- Jouini A., 2007: MgAl₂O₄ Spinel Laser Crystals: Pure and Ti-, Mn-, or Ni-Doped. Shaped Crystals, In: Fukuda T., Chani V.L., Advances in Materials Research, 8. Springer, Berlin, Heidelberg.
- Khanin Y.I., 1995: Principles of laser dynamics. Elsevier, Amsterdam, 407 p.
- Mainman T.H., 1960: Stimulated optical radiation in ruby. *Nature*, 187, 493–494.
- Nassau K., 2001: The physics and chemistry of color: the fifteen causes of color. 2nd ed. Wiley, New York, 481 p.
- Penzkofer A., 1988: Solid state lasers. *Progress in Quantum Electronics*, 12, 4, 291–427.
- Pugh-Thomas D., Walsh B.M. & Gupta M.C., 2010: Spectroscopy of BeAl₂O₄:Cr³⁺ with application to high-temperature sensing. *Applied Optics*, 49, 15, 2891–2897.
- Ristic S., Polic-Radovanovic S., Katavic B., Kutin M., Nikolic Z. & Puharić M., 2010: Ruby laser beam interaction with ceramic and cooper artifacts. *Journal of Russian Laser Research*, 31, 4, 380–389.
- Rossman G.R., 2017: Mineral Spectroscopy Server. <http://minerals.gps.caltech.edu/>, [30.10.2017].
- Schawlow A.L. & Townes C.H., 1958: Infrared and Optical Masers. *Physical Review*, 112, 6, 1940–1949.
- Silfvast W.T., 2004: Laser fundamentals. Cambridge University Press, New York, 625 p.
- Singh S.C., Zeng H., Guo C., Gopal R. & Cai W., 2012: Nanomaterials: Processing and Characterization with Lasers. Wiley, 777 p.
- Svelto O., 2010: Principles of Lasers, 5th ed. Springer, 620 p.
- Trindade N.M., Scalvi R.M.F. & Scalvi L.V.A., 2010: Cr³⁺ distribution in Al₁ and Al₂ sites of alexandrite (BeAl₂O₄: Cr³⁺) induced by annealing investigated by optical spectroscopy. *Energy and Power Engineering*, 2, 1, 18–24.
- Yorulmaz I., Beyatli E., Kurt A., Sennaroglu A. & Demibas U., 2014: Efficient and low-threshold Alexandrite laser pumped by a single-mode diode. *Optical Materials Express*, 4, 44, 776–789.